AD-A108 012 AIR FORCE INST OF TECH WRIGHT-PATTERSON AFB OH F/G 4/2
GLOBAL WINDS, BY TRACKING METEOSAT WATER VAPOR PATTERNS.(U)
MAY 79 L R JOHNSON
UNCLASSIFIED AFIT-CI-79-286T-S NL

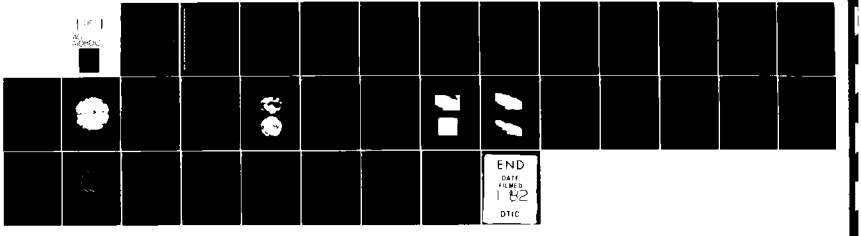

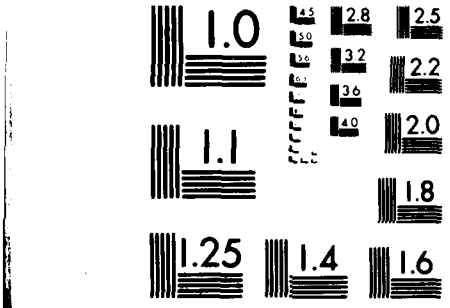

UNCLASS

SECURITY CLASSIFICATION OF THIS PAGE (When Data Entered)

REPORT DOCUMENTATION PAGE

READ INSTRUCTIONS BEFORE COMPLETING FORM

1. REPORT NUMBER: 79-286T-S	2. GOVT ACCESSION NO: AD A108012
3. RECIPIENT'S CATALOG NUMBER:	
4. TITLE (and Subtitle): Global Winds, by Tracking Meteosat Water Vapor Patterns.	5. TYPE OF REPORT & PERIOD COVERED: THESIS/DISSERTATION
	6. PERFORMING ORG. REPORT NUMBER:
7. AUTHOR(s): Larry Richard Johnson	8. CONTRACT OR GRANT NUMBER(s): Master's Thesis
9. PERFORMING ORGANIZATION NAME AND ADDRESS: AFIT STUDENT AT: Univ of Wisconsin-Madison	10. PROGRAM ELEMENT, PROJECT, TASK AREA & WORK UNIT NUMBERS:
11. CONTROLLING OFFICE NAME AND ADDRESS: AFIT/NR WPAFB OH 45433	12. REPORT DATE: May 1979
	13. NUMBER OF PAGES: 26
14. MONITORING AGENCY NAME & ADDRESS (if different from Controlling Office)	15. SECURITY CLASS. (of this report): UNCLASS
	15a. DECLASSIFICATION/DOWNGRADING SCHEDULE

LEVEL III

16. DISTRIBUTION STATEMENT (of this Report)

APPROVED FOR PUBLIC RELEASE; DISTRIBUTION UNLIMITED

DTIC ELECTE DEC 2 1981 S D H

17. DISTRIBUTION STATEMENT (of the abstract entered in Block 20, if different from Report)

23 NOV 1981

18. SUPPLEMENTARY NOTES

APPROVED FOR PUBLIC RELEASE: IAW AFR 190-17

FREDRIC C. LYNCH, Major, USAF
Director of Public Affairs
Air Force Institute of Technology (ATC)
Wright-Patterson AFB, OH 45433

19. KEY WORDS (Continue on reverse side if necessary and identify by block number)

20. ABSTRACT (Continue on reverse side if necessary and identify by block number)

ATTACHED

DD FORM 1 JAN 73 1473 EDITION OF 1 NOV 65 IS OBSOLETE

UNCLASS 012200

SECURITY CLASSIFICATION OF THIS PAGE (When Data Entered)

81 11 30 018

DTIC FILE COPY

ABSTRACT

Geostationary satellite images of water vapor fields show promise as tracers of air motion, even in cloud-free regions. In this study, wind vectors are calculated, using Meteosat water vapor images as passive tracers of air motion. 781 individual wind vectors are obtained for the earth-disc view seen by Meteosat; this is nearly total and homogeneous spatial coverage, even in clear regions. A sample of these vectors is compared to radiosonde winds, yielding accuracies at least as good as from cloud-drift winds.

These winds represent tropospheric motions, but more precise height assignments are needed. Useful heights can be estimated for large scale area averages and for macroscale horizontal depictions, but they are not adequate for the vertical placement of wind vectors in baroclinic zones or in sub-synoptic activity. Application of the water vapor sensor on the other geostationary satellites could allow accurate stereographic height estimates.

GLOBAL WINDS, BY TRACKING METEOSAT WATER VAPOR PATTERNS

by

LARRY RICHARD JOHNSON

A thesis submitted in partial fulfillment
of the requirements for the degree of

MASTER OF SCIENCE

(Meteorology)

at the

UNIVERSITY OF WISCONSIN - MADISON

1979

APPROVED:

Verner E. Suomi, Professor
Department of Meteorology
May 30, 1979

I DEDICATE THIS GRADUATE EFFORT --

To my loving wife, Ruth, whose ever-present smile, faith, and encouragement have made today bearable, and tomorrow something to look forward to;

And to my children, Julie and Heather, whose presence has given my life great pride and meaning.

ACKNOWLEDGMENTS

I would like to express my appreciation to the Department of Meteorology staff for a graduate education second to none. Thanks also to Professor Verner E. Suomi, for the high honor of studying under his supervision. His inspiration and foresight have always impressed me. Thanks also to Professor Donald R. Johnson for constructively reviewing my manuscript, and to Professor Eberhard W. Wahl who gave me much sound advice when I needed it.

A special thanks to Tom Haig, who "made things work" when I needed the help; to Dr. Fred Mosher, who was always willing to take time to help me; to Dr. David Suchman, for his capable advice during the final thesis review; and to Dee Cavallo, the real hero of McIDAS operations. To J. T. Young, Tom Whittaker, Vicki Epps, and Brian Auvine, also go my sincere appreciation.

My good friend E. J. Hopkins is singularly responsible for keeping my spirits up while in graduate school; Ron Townsend, Lou Luces, and Marge Hopkins were my mentors as well as cherished friends. My officemates and other friends also made my life richer.

The biggest thanks go to my family, for their unending tolerance of my long hours of absence and studying. They have been the most understanding family a person could have.

This research was made possible by the Air Force Institute of Technology (AFIT), and by NOAA Grant 04-6-158-44087.

ABSTRACT

Geostationary satellite images of water vapor fields show promise as tracers of air motion, even in cloud-free regions. In this study, wind vectors are calculated, using Meteosat water vapor images as passive tracers of air motion. 781 individual wind vectors are obtained for the earth-disc view seen by Meteosat; this is nearly total and homogeneous spatial coverage, even in clear regions. A sample of these vectors is compared to radiosonde winds, yielding accuracies at least as good as from cloud-drift winds.

These winds represent tropospheric motions, but more precise height assignments are needed. Useful heights can be estimated for large scale area averages and for macroscale horizontal depictions, but they are not adequate for the vertical placement of wind vectors in baroclinic zones or in sub-synoptic activity. Application of the water vapor sensor on the other geostationary satellites could allow accurate stereographic height estimates.

TABLE OF CONTENTS

LIST OF FIGURES

LIST OF TABLES

I. Introduction.

Since the development of the geostationary satellite in the 1960's, successful demonstrations of accurate cloud tracking have been demonstrated, notably by Suomi and Parent (1967), Smith and Phillips (1972), Bauer (1976), Suchman and Martin (1976), and others. Useful cloud-motion vectors are now provided on a large scale, both operationally and in a research mode, to supplement conventionally-obtained observations. Generally, in areas where these cloud-motion observations can be derived, the spatial and temporal resolution of the winds are quite adequate. Gaps still do exist in cloud-free areas, suggesting an overall sampling bias toward stronger winds, upward motion, or cloud-covered areas, (Hinton, 1977). This bias, or spatial aliasing, probably extends to geographic regions which favor the presence or formation of clouds, such as normal subtropical jet source regions.

Water vapor fields, derived from 6.7 micrometer water vapor channel radiometers aboard the Nimbus polar orbiting series of meteorological spacecraft, have been used for indicating the upper tropospheric field of motion, (Allison et al, 1972; Steranka et al, 1973; and Mosher, 1976). In fact, the motion of these fields can be traced through time, providing wind measurements in cloud-free areas void of upper-air weather observations. This is important, since much of the earth's area falls into this category -- particularly the subtropics, where the belt between 30 degrees north and south latitude

has comparatively fewer observations.

This study explores a new resource -- the application of a 5.7-7.1 micrometer water vapor sensor to a European geostationary meteorological satellite, Meteosat-1. The sensor offers increased spatial (5 km vice 25 km), and temporal (1/2 hr vice 12 hrs), resolution over the Nimbus data, and provides the first opportunity to continuously observe these high resolution water vapor fields from a geostationary perspective, (36,000 km above the crossing point of the equator and the Greenwich meridian). This is particularly useful in tropical regions, where polar orbiting satellites provide their poorest area sampling.

The second chapter will document this research effort: Section A introduces the satellite-sensor combination, and Section B describes the image data used for the study. Section C focuses on the creation of a wind vector data set from the water vapor images. It will demonstrate that accurate winds are obtained over virtually the entire viewing area of the satellite, regardless of cloud amount. Further, they are obtained from a weather-independent observation scheme, so they do much to approach a zero-bias wind data set. This lends the data to statistical averaging for climatological use. In Section D, the question of height assignments is treated. Incorrect height estimates in a hyperbaroclinic zone would probably negate the effects of increased data coverage; it is therefore critical to seek as precise an estimate of height as possible. Three examples of differing height accuracy requirements will be illustrated: First, where a

knowledge of the water vapor weighting function is sufficient; second, where image calibration and a climatological standard atmosphere will provide a reasonable mapped height field; and third, where intense baroclinicity, sub-synoptic severe weather events, or small-scale image analysis require height resolution not currently available. New methods should be investigated to improve upon current height accuracies. As an example, the application of the water vapor sensor to other geostationary meteorological satellites could provide the opportunity for accurate real time stereographic calculations of image heights.

The final chapter will summarize the evidence to show why the water vapor-derived winds have such potential value for future generations of geostationary meteorological platforms. The possibility of global winds at accurately-known heights would be of great benefit for meteorological applications -- particularly considering the recently increased emphasis placed on understanding the global climate.

II. The Wind Vector Calculations.

Figure 1 is a Meteosat water vapor image obtained in April 1978. This startling perspective of the atmosphere reveals a filmy water vapor continuum, particularly in the mid- to high-latitudes -- in which many different scales and waveforms coexist and intertwine. There also appears to be occasional coupling between tropical convective activity and mid-latitude storm systems. In general, the atmosphere appears quite complex, and with interactions not normally seen using other forms of data.

A. The Satellite-Sensor Combination.

Meteosat-1 is one component of a global network of five geostationary meteorological satellites arranged in near-symmetric equatorial orbit, but is the only one with a water vapor channel. It was launched on 23 November 1977 from Cape Canaveral, Florida, and is operated by the European Space Agency, (ESA). Located approximately 36,000 km above the equator and the Greenwich meridian, it overlooks all of Africa and the Atlantic Ocean, most of Europe, and eastern South America. Appendix A describes Meteosat-1 system details, and strikes comparisons with the U. S. GOES satellites.

The system component of interest here is the 5.7-7.1 micrometer water vapor absorption channel. This channel senses tropospheric water vapor emissions, and produces mapped images for the earth's disc viewed by the satellite. Figure 2 shows the atmospheric emission spectrum, notably the region sampled by the water vapor sensor.

METEOSAT 1978 MONTH 4 DAY 10 TIME 1155 GMT (NORTH) CH. WV
NOMINAL SCAN/PROCESSED SLOT 24 CATALOGUE 1001710051

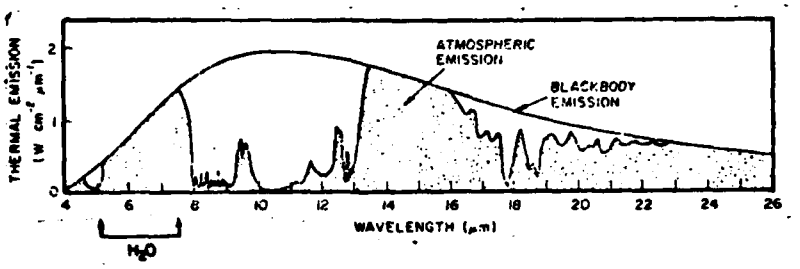

Figure 2. Spectral distribution of radiation emitted by the atmosphere compared to that emitted by a black body at the same temperature. Note the water vapor emission region sampled by the 5.7-7.1 micrometer radiometer. (From Coulson, 1975)

The energy received at the sensor will be representative of the mean black body temperature of the water vapor emissions. Since this involves a layer of moisture, some emissions will be colder where the layer is at higher altitudes, and some will be warmer when the layer is lower. The vertical distribution of moisture is not likely to be homogeneous; rather, it will tend to be concentrated along selected isentropic surfaces. The temperature seen by the sensor need not be at the mid-point of the moisture layer.

In the water vapor images, bright scenes will represent colder temperatures, thereby indicating high, dense moisture fields, (and often cloudiness). Conversely, dark areas will represent warmer temperatures from lower levels, suggesting shallow moisture layers. Since this water vapor mass tends to be conservative, streaks of water vapor can be traced as they move along or through their isentropic paths. The time rate of change of a moisture field would indicate rising motion for increasing brightness, and subsidence for decreasing brightness.

B. The Data Set.

This study was based on a data set contributed by J. Morgan of ESA (Houghton and Suomi, 1978). Ten raw data tapes of water vapor (5.7-7.1 micrometer) and "window" (10.5-12.5 micrometer) images for the period 2100 GMT 24 April to 0130 GMT 25 April 1978 comprised the data set, and all wind vector calculations were made using three consecutive water vapor images centered on 2300 GMT. This also provided relatively easy comparison with 0000 GMT radiosonde data.

As figure 3 shows, the most striking feature of the water vapor, as compared to the window channel, is the continuous nature of the moisture fields. Mid- and high-tropospheric circulation patterns are suggested a priori from time-sequence water vapor images. Perhaps the most interesting meteorological features of this data are the large areas of moist high-tropospheric mass transport from equatorial regions deep into mid-latitude baroclinic disturbances. The water vapor images showed this clearly, but comparable infrared "window" images suggested it only after a preview was obtained from viewing the water vapor.

C. The Wind Calculation Method.

Modern interactive man-computer techniques lend themselves well to the quantitative investigation of geostationary satellite-produced images, so the interactive capability of the Man-Computer Interactive Data Access System (McIDAS), of the University of Wisconsin Space Science and Engineering Center (SSEC), was ideal as the prime investigative tool used for this study. The McIDAS system, (Suomi, 1975;

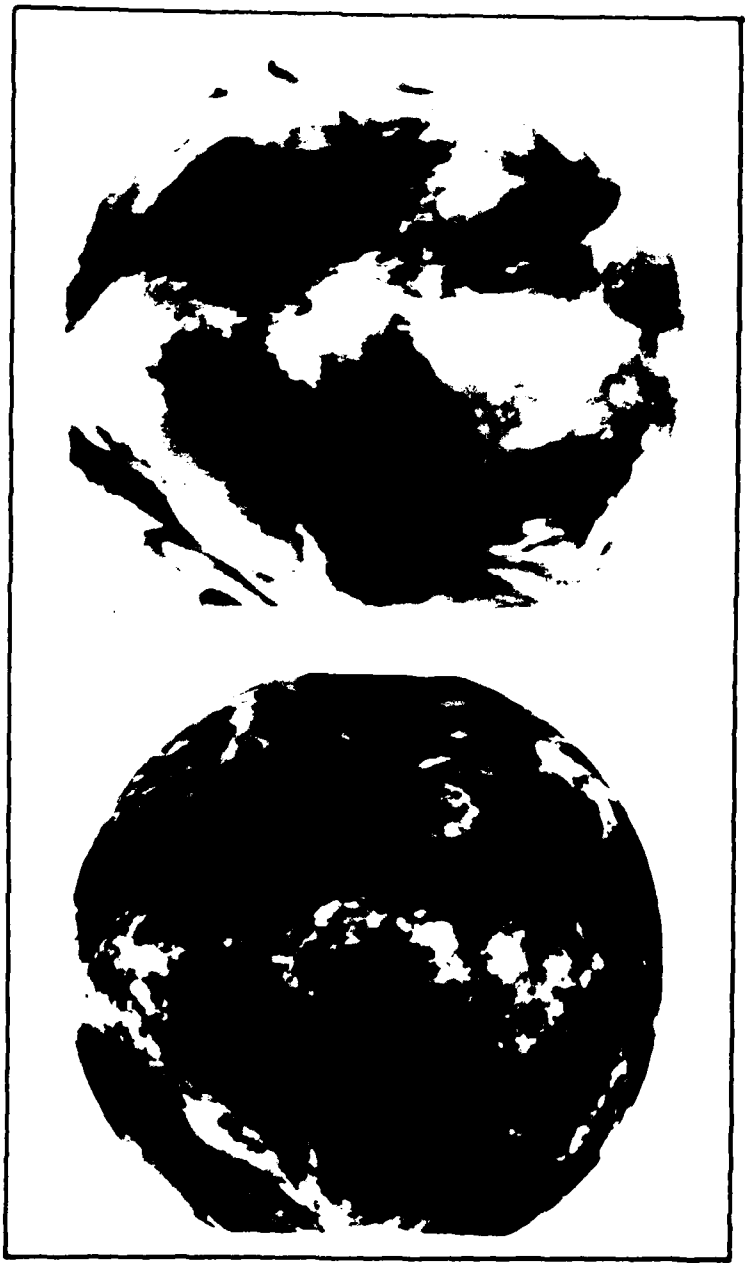

Figure 3. Comparison of the 5.7-7.1 micrometer water vapor imagery (top), with the coincident 10.5-12.5 micrometer "window" region imagery (bottom). Data are for 2300 GMT 24 April 1978.

Smith, 1975; Chatters and Suomi, 1975), is an interactive capability involving imagery storage, processing, and display on a mini/midi-size computer system. A meteorologist-operator, using a large repertoire of flexible commands, carries an image set through accurate navigation, enhancement, loop construction, and wind vector calculations, all the while viewing the product of his labors on a cathode ray tube, (CRT).

The McIDAS system was essentially developed around the U.S. ATS and GOES satellite programs, so certain dissimilarities in the Meteosat system had to be satisfied. The different scan and spin directions of the spacecraft, the dissimilar line count and timing, and the problems of accurate navigation without visual imagery, (a common mode when the water vapor channel is operative), are examples. After resolving these complications, calculation of wind vectors was begun, using the WINDCO system.

The WINDCO cloud tracking system on McIDAS has been amply documented, (Smith and Phillips, 1972; Chatters and Suomi, 1975; Smith, 1975). Studies by Bauer (1976), Suchman and Martin (1976), and others have shown that cloud drift winds can be as accurate as <u>in situ</u> measurements, such as radiosonde-derived winds.

Water vapor data form a passive tracer from which wind vectors can be derived. The process requires care, since water vapor fields, particularly in subsident regions, are quite "fuzzy" or "flat"; that is, they form a continuum, rather than a random array of discrete elements, and the gradient may be very slight. The tracking of features imbedded in this field takes on an element of subjectivity

not experienced when tracking low level discrete cumulus clouds. Image enhancement techniques were therefore required and used to bring out the fine structure of the water vapor.

Figure 4a is a close-up of the subtropical South Atlantic area. The image is "flat" because it has a low contrast ratio; the brightest and darkest returns occupy only 20% of the total possible brightness range, as shown in the brightness histogram of figure 4b. Image enhancement can "stretch" this across the total possible range to produce a greater apparent contrast between the darkest and brightest scenes, as figure 4c illustrates. Other options are available, such as greater enhancement of the darkest returns (figure 4d), or of the brightest ones.

The subjective nature of tracking the water vapor streaks and filaments required manual target identification, so the single pixel (SP) tracking method was used for all wind vector calculations. These calculations were done using a horizontal image resolution of 10 km. This was chosen because the 5 km basic resolution: (1) involved considerably more time and expense to process, and (2) had an erratic "grainy" or "noisy" appearance. This latter problem may have been a manifestation of interference patterns documented in the ESA Meteosat-1 Calibration Report, (ESA, 1979). At the time these data were collected, one regular pattern at a recurring wavelength of 2.5 picture elements, and one random white noise pattern had been identified through spectral analysis.

The selection of 10 km resolution data necessitated dividing the

Figure 4a. Original water vapor image without image enhancement.

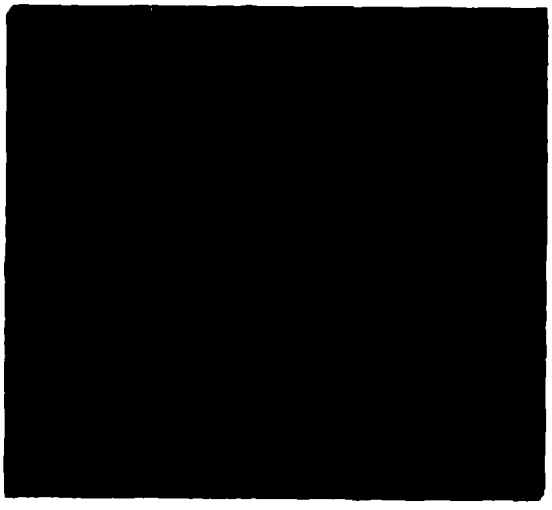

Figure 4b. Brightness histogram of image in figure 4a. Entire brightness range is compressed into 20% of the total possible range.

Figure 4c. Same as figure 4a, except image enhancement applied.

Figure 4d. Same as figure 4c, except stronger image enhancement applied to darkest scenes.

earth's disc into seven overlapping areas. The overlap allowed independent intracomparison of wind vectors calculated near the edges of each area, thereby providing an informal quality control mechanism as the wind vectors were calculated.

Based on experimentation, an objective of 100 edited winds per area was established as a minimum requirement to insure representativeness, sufficiency, and homogeneity of data coverage. Generally, no winds were calculated for earth-satellite angles greater than 55 degrees. Random comparisons between "window" and water vapor-derived wind vectors were made throughout the wind data set generation, and there was consistently good agreement between the two.

Finally, the seven areas were merged, and 1823 total vectors had been calculated, which were then temporally averaged to produce 911 point winds. These were further edited for quality and reproducability to a final 781 individual wind vectors for the full earth-disc view. More vectors could easily have been calculated.

Figure 5 shows this final water vapor-derived wind vector data set. There is nearly complete and homogeneous spatial coverage, regardless of geographical location or of cloud amount.

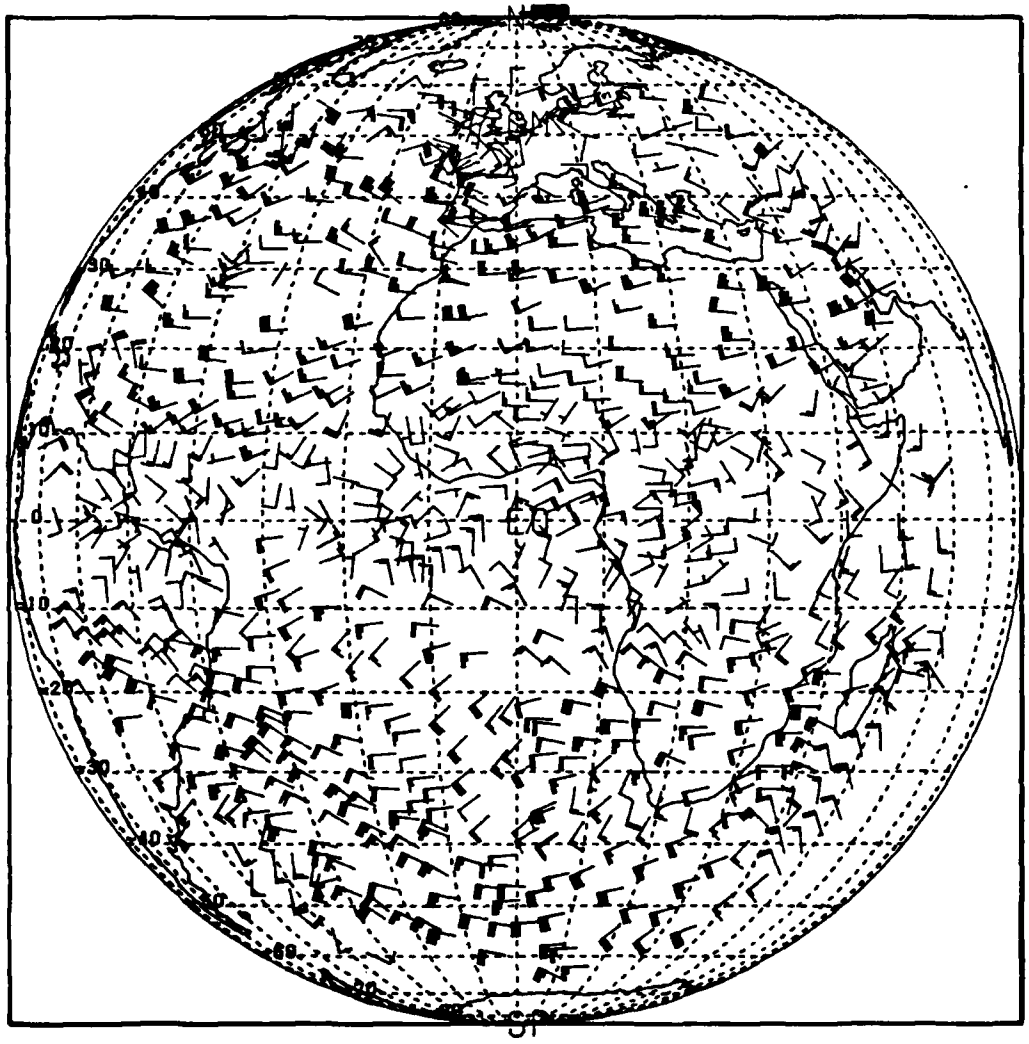

Figure 5. The final water vapor-derived wind set, plotted on the earth-disc viewed by Meteosat.

D. Wind Vector Quality and Limitations.

Statements concerning the accuracy of water vapor winds must consider the differences in vector heights caused by the varying altitudes and layer thicknesses of the tracked moisture fields. This is a more difficult problem than the similar task of assigning heights to cirrus or cumulus cloud-derived wind vectors. It can be approached with varying degrees of accuracy, depending on user applications. The following are three possible examples:

Example 1: Since procedures for tracking the water vapor images are similar to cloud-tracking procedures, the results of cloud-tracking quality assessments are worth noting. Bauer (1976) found that rms differences between cloud-drift and radiosonde winds were about 6.4 m/sec for total velocity. Suchman and Martin (1976) determined accuracies of 8.9 m/sec for cirrus cloud comparisons.

Using a radiosonde data-rich section of Europe, brief comparisons were made between the variable-level water vapor-derived wind set and three standard radiosonde levels, at 300, 400, and 500 mb. By assuming the water vapor winds were at the same level as the radiosonde data, the radiosonde level of best fit could be found. Table 1 summarizes this comparison: The 400 mb level provided the best fit to the water vapor data, with a mean rms difference of 6.9 m/sec for total velocities. This suggests that 400 mb is probably a practical height assignment for large-scale statistical studies involving mean values, rather than point-by-point comparisons. (If the water vapor heights were known accurately, they could then be compared to equiv-

TABLE 1

RADIOSONDE LEVEL OF BEST FIT TO THE WATER VAPOR DATA.

(Absolute rms differences (m/sec) between the variable-height water vapor wind field and each standard radiosonde level)

COMPARISON	$\overline{\Delta u}$	$\overline{\Delta v}$	$\overline{\Delta \text{total vel.}}$
300 mb radiosonde winds v.s. water vapor winds	7.6	5.9	9.6
400 mb radiosonde winds v.s. water vapor winds	4.6	5.1	6.9
500 mb radiosonde winds v.s. water vapor winds	6.1	5.6	8.2

alent-level radiosonde winds, and much smaller rms differences would be expected.)

Example 2: Large-scale horizontal mapping of the image height field can be accomplished through the use of radiometric image calibration data prepared by ESA, (Morgan, 1979; ESA, 1979). These data, in the form of a "calibration curve", (figure 6), permit conversion of radiometric image brightness values to black body temperatures. These temperatures can then be converted to height values through the use of a latitudinally-corrected standard atmosphere. This method relies on the principle of the water vapor weighting function, and assumes a fairly uniform distribution of moisture about the mean layer height. This is probably realistic in widespread subsident areas, but is incorrect in convective or baroclinic regions.

The technique was applied to the water vapor imagery, and the

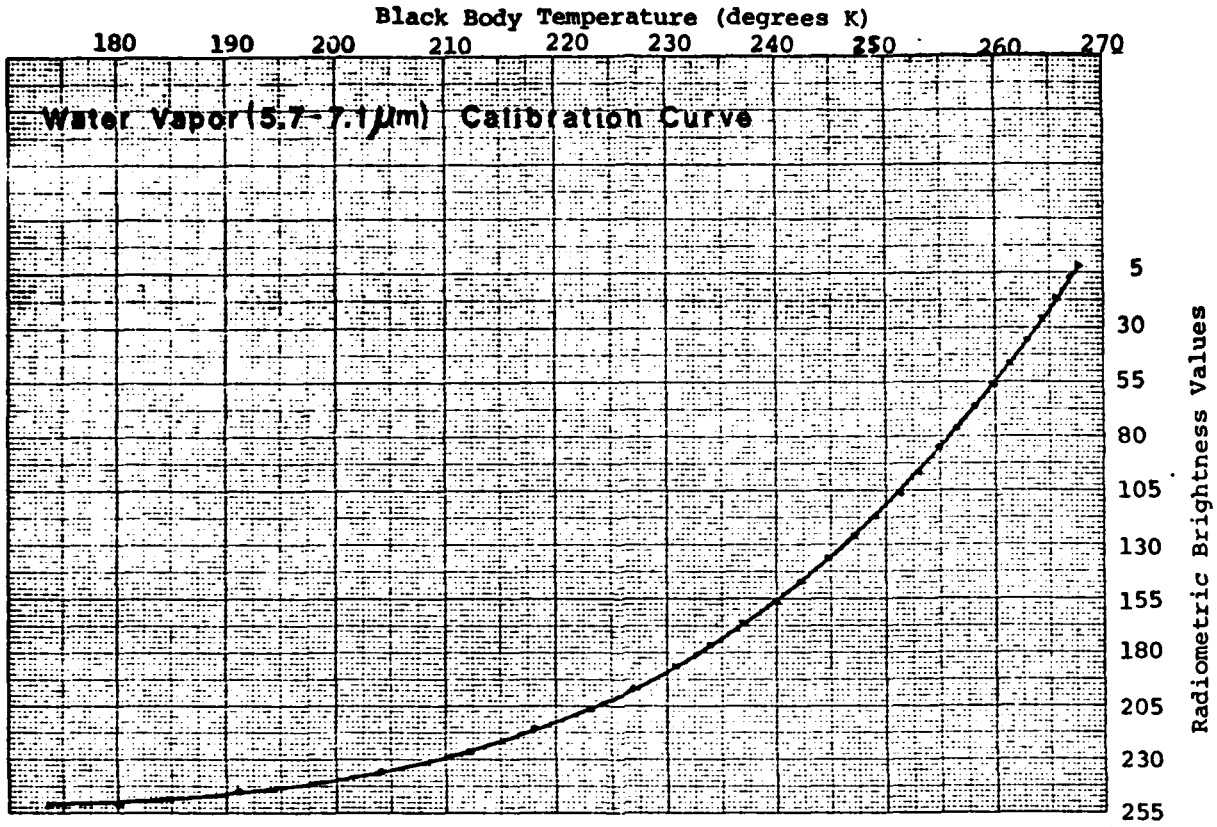

Figure 6. The 5.7-7.1 micrometer calibration curve for conversion of radiometric brightness values to Planck-function black-body temperatures. (From ESA, 1978)

resulting 2300Z image height depiction is shown in figure 7. This depiction, when compared to the image in figure 4, seems adequate as a large-scale, gross-resolution estimate, but little reliance could be placed on height values derived in active weather regions.

Example 3: For smaller-scale studies involving wind calculations at individual points, more precise height estimates are necessary. This is particularly true of hyperbaroclinic regions or subsynoptic severe storm systems. Wind vectors calculated in regions of strong vertical wind shear require improved height discrimination, since erroneous height assignments would likely negate the data's value. To demonstrate this point, a comparison was made of vertically-adjacent radiosonde levels over Europe. Using the 300, 400, and 500 mb level winds, a mean rms difference of 7.4 m/sec was found between consecutive levels. Much larger vertical wind shears would be expected in smaller scale hyper-baroclinic zones, which demonstrates the critical necessity for accurate height assignments to wind vectors generated in these areas.

Even the water vapor weighting function, (figure 8), affords no hope at all for assigning precise height values to strongly baroclinic systems. The highly non-homogeneous distribution of moisture in baroclinic systems, coupled with the broadness of that weighting function, limit its application to large-scale gross-resolution estimates of image heights.

It appears, then, that large-scale gross resolution height assignments can be made for the water vapor wind data, but based on

Figure 7. Calculated image height field, averaged to the nearest 100 mb layer.

LEGEND:

200 mb 300 mb 400 mb 500 mb 600 mb

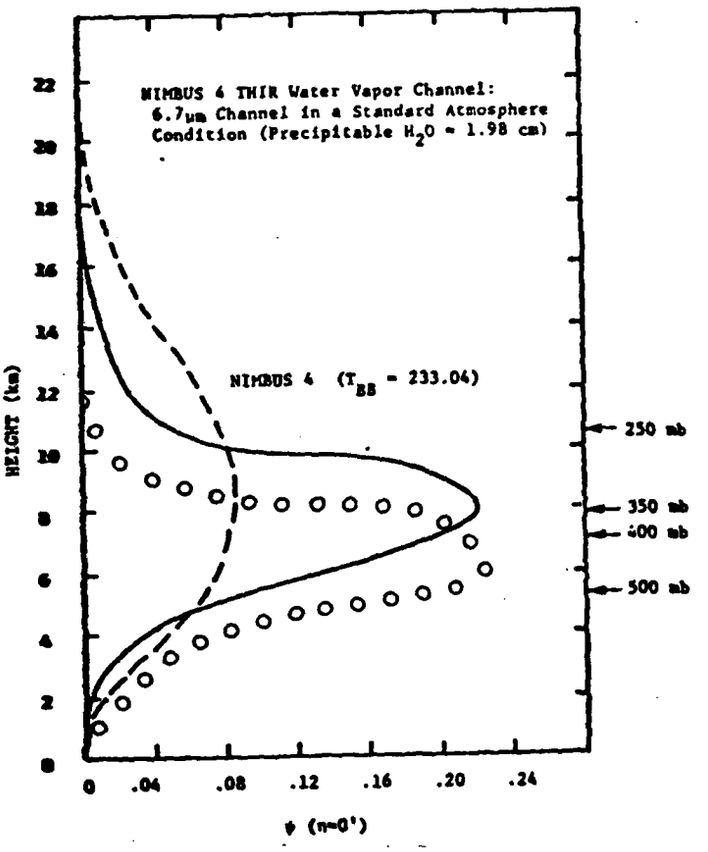

Figure 8. A plot of the weighting function, ψ, showing the atmospheric emission distribution contribution at various altitudes in the 6.7 micrometer channel.

——— mean layer profile

– – – – alternative possibility based on greater vertical distribution of the moisture.

o o o o alternative possibility based on lower-altitude moisture layer.

(From Steranka et al, (1973), with modifications)

these three examples, "meteorologically active" regions or sub-synoptic scale analysis will require a more sophisticated technique. If the data are to be given real-time use as a supplement to existing data sources, and if precise height assignments are necessary, some other means of providing it will have to be devised.

Application of the water vapor sensor to other geostationary meteorological satellites, for example, would permit real time use of the more accurate stereographic height determination technique, (Bryson, 1978).

III. Summary and Conclusions.

The water vapor-derived wind set in figure 5 speaks for itself. This type of continuous data coverage on a global scale would have a major impact on meteorology. These observations have been derived without regard to existing cloud amounts, and provide nearly total and homogeneous spatial coverage of the tropospheric area viewed by Meteosat. Accuracies of these vectors, compared to radiosondes, appear to be at least as good as cloud-tracked winds. Further, they are free of the spatial aliasing found in cloud-tracking, and of localized geographic bias. This lends the water vapor wind data to climatological averaging, since there is little likelihood of aliasing the statistical conclusions. The key problem, however, is that of adequate height determination. In areas of large vertical wind shear or non-homogeneous moisture distribution, heights are particularly hard to estimate. For real time data application, this is significant.

Routine, continuous water vapor observations, from the global system of geostationary satellites, would provide an excellent diagnostic capability over those portions of the earth where few observations now exist. The tropics are especially important, since they form the "heat engine" which drives the global circulation system. The ability to continuously monitor this region can bring meteorologists closer to understanding the earth's climate.

Even in mid-latitudes, water vapor-derived winds can improve

upon existing data. Figure 1 clearly illustrates the fine structure of mid-latitude hyperbaroclinic zones. Water vapor winds can be selectively calculated at sufficient data density to provide a more refined description of these zones' structures. If the height of each vector could be determined accurately, a high-resolution three-dimensional representation could be constructed.

No method currently exists for precise real time calculations of water vapor image heights in highly baroclinic areas. Stereographic techniques might be a solution to this problem -- an option which would be available if the water vapor sensor were included in future upgrades to the total system of geostationary meteorological satellites.

This study has shown that the ability to calculate clear-sky wind vectors, the absence of a spatial aliasing problem, the potential for increased discrimination of hyperbaroclinic zones, and the opportunity for more accurate image height estimates, all provide excellent reasons why the water vapor sensor has such potential for future generations of geostationary meteorological satellites.

APPENDIX A

Meteosat-1 Details

(*) indicates that comparative GOES data follows.

General

Program Manager	European Space Agency, (ESA)
Controller	European Space Operations Center, (ESOC)
Central Communications Site	Michelstadt, F. R. Germany

Vehicle

Launch Date	0130 GMT, 23 November 1977
Launch Site	Cape Canaveral, Florida, USA
Booster	Delta 2914
Life Expectancy	3 years
Apogee	35,692 km
Perigee	34,913 km
Subpoint	0 degrees latitude/0 degrees longitude
Spin Rate	100 rpm
*Spin Direction	East to West
*Scan Period	25 minutes
*Scan Direction	South to North
Image Interval	30 minutes

Sensors	Visible	IR(window)	IR(water vapor)
*Radiometer (micrometers)	0.4-1.1	10.5-12.5	5.7-7.1
*Resolution (kilometers)	**2.5	5.0	5.0
*Scan Lines/Image	***5000	2500	2500
Elements/Line	5000	2500	2500

Notes

** Resolution is achieved through 2-channel parallel scanning. Water vapor channel is activated at the expense of one of these channels. Visible resolution then decreases to 5.0 km north-south (across scan), but remains 2.5 km east-west, (along scan).

*** May be reduced to 2500 scan lines/image. See note (**).

U.S. GOES Comparisons

Vehicle

*Spin Direction	West to East
*Scan Period	18.2 minutes
*Scan Direction	North to South

Sensors	Visible	IR(window)
*Radiometer (micrometers)	0.55-0.70	10.5-12.6
*Resolution (kilometers)	1	8
*Scan Lines/Image	****14,568	1,821

Notes

**** Resolution is achieved through 8-channel parallel scanning.

Reference: ESA, (1978, 1979); Morel et al, (1978); Morgan, (1978); Gatland, (1978a, 1978b); Corbell et al, (1976).

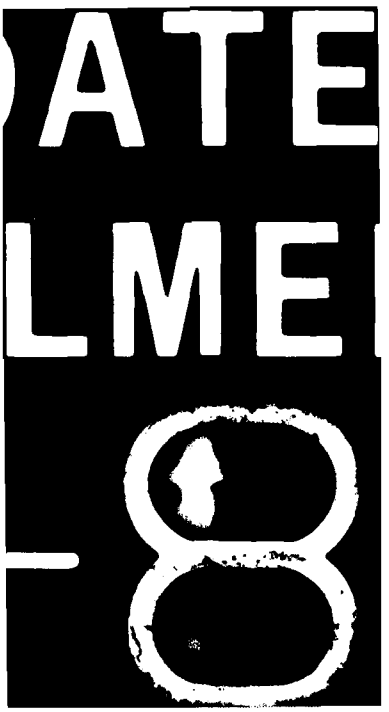
ATE
LME
8